Theoretical Study of *o*-Quinone Complexes of Iron

DOUGLAS J. GORDON and RICHARD F. FENSKE*

Results of molecular orbital calculations on a seven-membered redox series of tris(*o*-quinone)iron complexes are presented and compared to those of the related chromium series. Predictions of the ground-state electronic configuration are made on the basis of an occupation-weighted sum of 1-electron eigenvalues of the valence molecular orbitals (MOs) for the members of the series. Comparisons are made between the total spin obtained from magnetic measurements and that obtained from the calculations. Good agreement is obtained for the 3+ iron complex, but the 3− iron complex is suggested to be worthy of further investigation. There is a smooth inversion of the metal- and the ligand-centered MOs as the seven-membered redox series is traversed owing to the relatively greater destabilization of the 3d orbitals of the iron as compared to the case of the ligand orbitals. The calculated charges on the iron and ligands are most consistent with a model for these complexes in which the charge on the iron remains constant and electrons are added to or removed from the ligands as the complexes are reduced or oxidized, which is the same result as that obtained for the chromium series. A good agreement is obtained between the calculated and the observed UV–visible spectra of the neutral and 3− iron complexes. By comparison of members of the iron series to those of the related chromium series, it is shown that the 3d orbitals of iron are more stable than the 3d orbitals of chromium for complexes having the same charge or the same number of electrons. Such comparisons show no evidence for the iron complexes being less stable thermodynamically than their chromium counterparts. Comparison of the 3− complexes of iron and chromium convincingly shows why the former complex exhibits an intense absorption in the visible region of the spectrum assignable to a ligand to metal charge-transfer transition and the later complex does not. From a bonding point of view or with reference to the relative energies of the MOs, it is shown that an iron complex of overall charge *n* most nearly resembles a chromium complex of overall charge *n* + 2 rather than the isoelectronic chromium complex of overall charge *n* − 2.

Introduction

Complexes of *o*-quinone ligands with transition metals have been the object of considerable interest in the past few years.[1-4] *o*-Benzoquinone (hereafter referred to as BQ) undergoes a series of 1-electron reductions to form the monoanionic *o*-benzosemiquinone (SQ) and the catecholate (CAT) dianion. *o*-Quinone transition-metal complexes are usually rich in oxidation–reduction chemistry, exhibiting an abundance of oxidation states. For example, the tris complex of 9,10-phenanthrenequinone (9,10-phenQ)[5] with chromium exhibits cyclic voltammetry half-waves corresponding to a seven-membered series with the overall charge on the complex ranging from 3+ to 3−.[6]

Although tris(*o*-quinone) complexes of iron are known with charges of 3+, 0, and 3−, e.g., $[Fe(9,10\text{-phenBQ})_3]^{3+}$,[7] tris-(3.5-di-*tert*-butyl-*o*-benzoquinone)iron $(Fe(3,5\text{-DBSQ})_3)$,[8] and $[Fe(CAT)_3]^{3-}$,[1,9] we are unaware of any reports of complexes of intermediate charge. Attempted reduction of the neutral iron complexes of 9,10-phenQ, 3,5-DBQ, and tetrachloro-1,2-benzoquinone (*o*-Cl$_4$Q) by cyclic voltammetry leads to ligand dissociation showing only irreversible waves with cyclic

voltammograms corresponding to the free quinone after 1 h.[6] The difference in the behavior of the tris(*o*-quinone) complexes of iron and chromium is attributed by these authors to the ligands being more tightly bound in the chromium complexes and to the kinetic stability to Cr^{3+}.

In the previous paper[10] we have presented the results of our molecular orbital calculations on the seven-membered redox series $[Cr(BQ)_3]^{3+}$, ..., $[Cr(CAT)_3]^{3-}$ using a nonempirical method known as the Fenske–Hall method.[11] It is the purpose of this paper to present the results of our calculations on the analogous iron system, e.g., $[Fe(Q)_3]^n$ (Q = *o*-quinone) for *n* ranging from 3+ to 3− in unit steps. The effect that varying the overall charge on the complex has on its electronic structure and bonding properties will be presented.

Method

The Fenske–Hall method is a nonempirical molecular orbital method and has been described previously.[11] It is important to note that, because the method uses no adjustable parameters, the final results depend only upon the choice of the atomic basis sets and molecular geometry. The basis functions were chosen as in ref 10. The atomic basis functions for iron correspond to the M(II) functions of Richardson et al.[12] and were chosen on the basis of the charge calculated for iron.

Molecular geometries were taken from published crystal structures when available. The CAT coordinates were obtained from the structure of $K_3[Fe(CAT)_3]\cdot1.5H_2O$ by Raymond et al.[1] The SQ positional parameters were derived by analogy from those used in the chromium calculations. The intraligand bond distances and angles were identical with those used in the chromium case and were taken from the structure of $[Cr(3,5\text{-DBSQ})_3]$[13] by replacement of the *tert*-butyl groups by hydrogens. The Fe–O bond distance was obtained by considering the difference in the covalent radii of Cr and Fe. Calculations were performed on Fe(SQ)$_3$ in which the Fe–O bond length and the O–Fe–O ligand bite angle were varied; the results were virtually identical with those presented here, indicating that the results of the calculations are not dependent on small variations in the chosen

(1) Raymond, K. N.; Isied, S. S.; Brown, L. D.; Fronczek, F. R.; Nibert, J. H. *J. Am. Chem. Soc.* **1976,** *98,* 1767-1774.
(2) Brown, D. G.; Johnson, W. L., III. *Z. Naturforsch., B: Anorg. Chem., Org. Chem.* **1979,** *34B,* 712-715.
(3) Buchanan, R. M.; Kessel, S. L.; Downs, H. H.; Pierpont, C. G.; Hendrickson, D. N. *J. Am. Chem. Soc.* **1978,** *100,* 7894-7900.
(4) For a recent review see Pierpont, C. G.; Buchanan, R. M. *Coord. Chem. Rev.,* in press.
(5) Because *o*-quinone ligands are "noninnocent" assigning oxidation states in their complexes can be difficult. Hereafter, when no statement about oxidation state is meant to be implied, a Q appears in the abbreviated form of the ligand, whereas if BQ, SQ, or CAT appears, this implies the ligand is of benzoquinone, semiquinone, or catecholate type, respectively.
(6) Downs, H. H.; Buchanan, R. M.; Pierpont, C. G. *Inorg. Chem.* **1979,** *18,* 1736-1740.
(7) Crowley, P. J.; Haendler, H. M. *Inorg. Chem.* **1962,** *1,* 904-909.
(8) Razuvaev, G. A.; Shal'nova, K. G.; Abakumova, L. G.; Abakumov, G. A. *Bull. Acad. Sci. USSR, Div. Chem. Sci. (Engl. Transl.)* **1977,** 1512-1515; *Izv. Akad. Nauk. SSSR, Ser. Khim.* **1977,** 1642-1645.
(9) Anderson, B. F.; Buckingham, D. A.; Robertson, G. B.; Webb, J.; Murray, K. S.; Clark, P. E. *Nature (London)* **1976,** *262,* 722-724.

(10) Gordon, D. J.; Fenske, R. F. *Inorg. Chem.,* preceding paper in this issue.
(11) Hall, M. B.; Fenske, R. F. *Inorg. Chem.* **1972,** *11,* 768-775.
(12) Richardson, J. W.; Nieupoort, W. C.; Powell, R. R.; Edgell, W. F. *J. Chem. Phys.* **1962,** *36,* 1057-1061.
(13) Sofen, S. R.; Ware, D. C.; Cooper, S. R.; Raymond, K. N. *Inorg. Chem.* **1979,** *18,* 234-239.
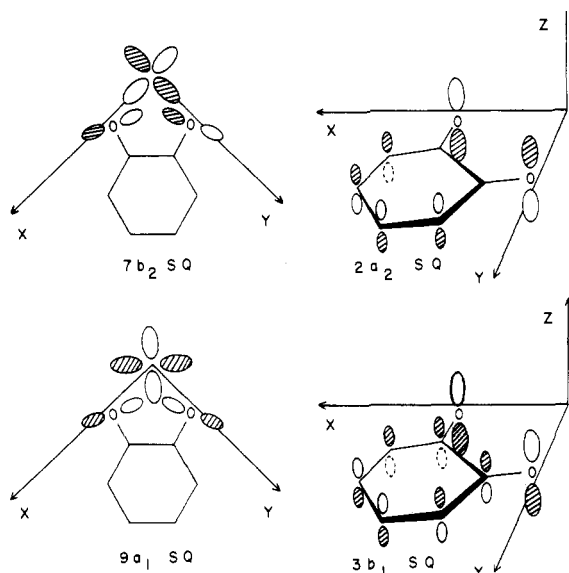
Figure 1. Schematic representation of the *o*-semiquinone (SQ) basis orbitals that contribute to the valence MOs of the complexes considered here. All SQ ligands shown lie in the *XY* plane. Shaded regions represent areas where the sign of the wavefunction is negative. For neutral BQ the HOMO is the $9a_1$ orbital and the LUMO is the $3b_1$ orbital.

geometry. The intraligand bond distances and angles for the BQ ligand were chosen to be the same as in free BQ[14]. The Fe–O bond distance was chosen by covalent radii considerations in a manner analogous to that used in the chromium calculations. For the complexes of intermediate charge, for which no crystal structures were available, the calculations were performed with use of ligands of two different types by analogy with our results on the chromium series.

Results and Discussion

Free Ligands. Figure 1 shows how the $7b_2$, $9a_1$, $2a_2$, and $3b_1$ orbitals on the SQ ligand in the *XY* plane interact with the iron. The position of the oxygen atoms is indicated by an O, all other vertices are assumed to be occupied by carbon atoms. The hydrogen atoms have been omitted since they make no significant contribution to these orbitals. The symmetry labels are taken from the C_{2v} point group. The results are virtually identical for free BQ or CAT so only those for SQ are shown here. In unshaded orbital lobes the sign of the wave function is positive while in shaded regions the wave function's sign is negative.

The $7b_2$ orbital for SQ interacts with the $d_{x^2-y^2}$ orbital on iron in a σ fashion as shown in Figure 1. The $7b_2$ orbital is localized on the two ortho oxygens and is filled in the free molecule, representing an oxygen lone pair. The interactions of the $9a_1$, $2a_2$, and $3b_1$ orbitals on the *o*-quinone ligand with the central metal are pictured in Figure 1 and described in ref 10. It is helpful to recall that the $9a_1$ orbital also interacts with the metal in a σ fashion while the $2a_2$ and $3b_1$ orbitals interact with iron in a π fashion.

The Configuration Problem. When one sets out to perform electronic structure calculations, the question of which electronic configuration gives rise to the lowest energy or ground state naturally arises. A proper theoretical interpretation of these tris(*o*-quinone)iron systems should be in accord with the experimental facts. To facilitate the discussion of our results, it is useful to first summarize the results of magnetic susceptibility and EPR experiments on the complexes that have been characterized.

For [Fe(9,10-henQ)$_3$]$^{3+}$ Crowley and Haendler[7] report values for the magnetic moment of approximately 6 μ_B, which

is very near the value of 5.92 μ_B for the spin-only moment for 5 unpaired electrons. On the basis of the magnetic data and the small shift in the C–O stretching frequency they formulate this compound as a high-spin Fe(III) bonded to three 9,10-phenBQ ligands.

A number of different values have been obtained for the effective magnetic moment of the neutral [Fe(3,5-DBQ)$_3$] compolex.[2,3,15] Brown and Johnson have obtained a value of 3.8 μ_B for the μ_{eff} of [Fe(3,5-DBQ)$_3$] in solution at room temperature. Buchanan et al. have performed temperature-dependent magnetic susceptibility experiments on the [Fe-(3,5-DBQ)$_3$] complex, and their results show little dependence of μ_{eff} on temperature, with a value at room temperature of 2.95 μ_B. This is quite near the spin-only moment value for 2 electrons of 2.8 μ_B, and they formulate this complex as a high-spin Fe(III) antiferromagnetically coupled to three 3,5-DBSQ ligands, thus leaving 2 unpaired electrons.

In contrast to the case of the [Fe(3,5-DBQ)$_3$] complex, magnetic susceptibility measurements on the [Fe(9,10-phenQ)$_3$] and [Fe(*o*-Cl$_4$Q)$_3$] complexes at a variety of temperatures show substantial dependence of μ_{eff} on temperature.[3,16] The neutral [Fe(9,10-phenQ)$_3$] complex yields values for μ_{eff} at 285 and 4.2 K of 3.43 and 1.52 μ_B, respectively, while the [Fe(*o*-Cl$_4$Q)$_3$] complex gives μ_{eff} values of 3.96 and 2.14 μ_B at 285 and 4.2 K, respectively. Buchanan et al. propose that the magnetic moments at room temperature, which are considerably above the spin-only value for 2 unpaired electrons, contain contributions from higher spin states. They explain that the antiferromagnetic interaction for the 9,10-phenSQ and *o*-Cl$_4$SQ ligands might be weaker than for 3,5-DBSQ due to a greater delocalization of the unpaired spin on the ligands. The fact that the magnetic moment falls well below the spin-only value for 2 electrons at low temperature for the [Fe(9,10-phenQ)$_3$] and [Fe(*o*-Cl$_4$Q)$_3$] complexes is explained as being due to intermolecular interactions in the solid that are absent when the bulky *tert*-butyl groups are present.

For the [Fe(CAT)$_3$]$^{3-}$ complex Anderson et al.[9] report that the results of variable-temperature magnetic susceptibility experiments indicate that there are 5 unpaired electrons. EPR experiments on aqueous [Fe(CAT)$_3$]$^{3-}$ at 77 K give a signal centered at $g = 4.3$, which has been assigned to high-spin Fe^{3+}[9,17] and also give a broad low-intensity signal of unknown origin centered at $g = 2.3$.

For the neutral [Fe(3,5-DBQ)$_3$] complex Buchanan et al.[3] report that they were unable to obtain an EPR signal on powdered samples in the temperature range 77–300 K; this they attribute to zero-field splitting of the $S = 1$ ground state. Brown and Johnson report observing a broad EPR signal centered at $g = 2.05$ for aqueous [Fe(3,5-DBQ)$_3$] at 77 K.

Figure 2 presents the results of our calculations on several alternative electronic configurations of the neutral [Fe(SQ)$_3$] complex. In this figure, as for all subsequent molecular orbital diagrams, a common energy scale in electronvolts appears on the left side. The molecular orbital diagrams are presented with the energies of the iron basis functions in the left-hand column, those of the ligand basis orbitals in the right-hand column, and the eigenvalues of the molecular orbitals (MOs) in the center column. All occupied MOs beginning with the Fe–SQ σ-bonding orbitals are shown as well as the lowest (few) unoccupied molecular orbital(s) (LUMO). The symmetry labels for the MOs are taken from the D_3 point group symmetry of the molecule. The electronic configuration is indicated at the top of each column and is presented schematically

(14) Macdonald, A. L.; Trotter, J. J. *J. Chem. Soc., Perkin Trans. 2* **1973**, 476–480.

(15) Raymond, K. N., private communication.

(16) Buchanan, R. M.; Downs, H. H.; Shorthill, W. B.; Pierpont, C. G.; Kessel, S. L.; Hendrickson, D. N. *J. Am. Chem. Soc.* **1978**, *100*, 4318–4320.

(17) Audeef, A.; Sofen, S. R.; Bregante, T. L.; Raymond, K. N. *J. Am. Chem. Soc.* **1978**, *100*, 5362–5370.
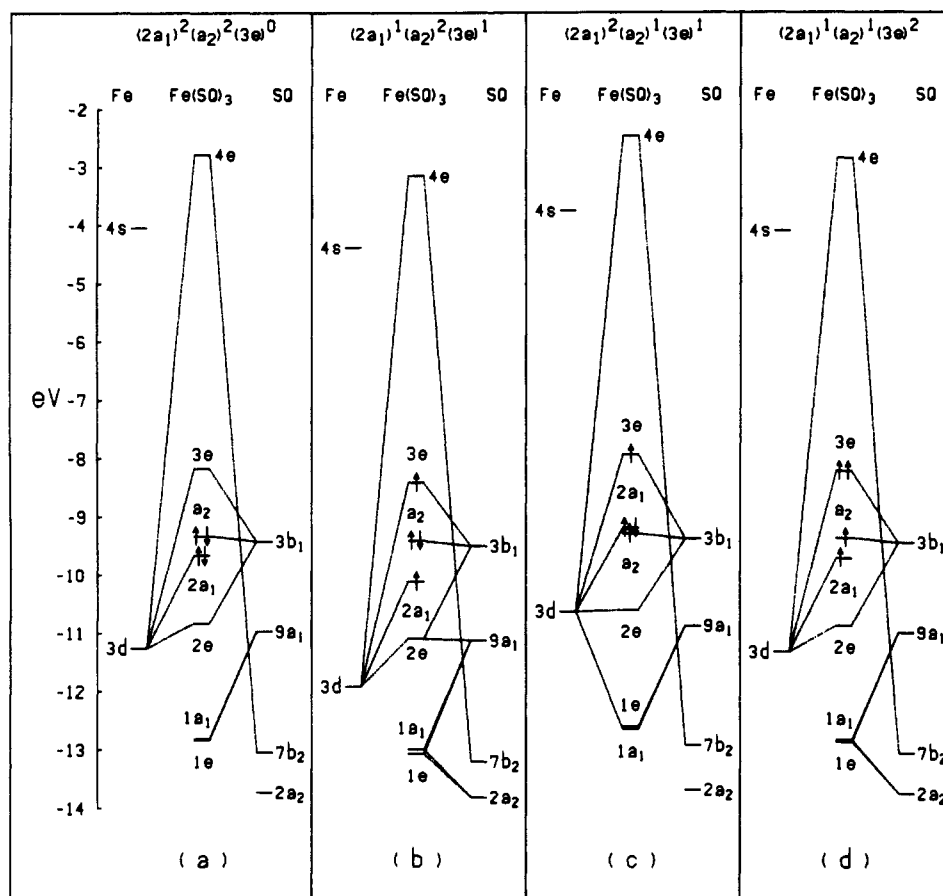
Figure 2. Molecular orbital diagrams for alternative configurations of the [Fe(SQ)₃] complex. The electronic configuration appears at the top and is presented schematically by arrows representing electrons. Arrows with the same direction represent electrons having the same spin. All MOs below those containing arrows are completely filled. See text for an explanation of symmetry labels. Where an e label appears without (1) or (2) appended, the MO is doubly degenerate.

within the MO diagram by arrows representing electrons. Arrows with the same direction represent electrons with the same spin, while arrows with opposite direction represent electrons of opposite spin. All MOs below those indicated by arrows are assumed to be completely filled, while those above are empty.

As shown in Figure 2 the 4s orbital of iron is much higher in energy than the 3d orbitals. The 4p orbitals (not shown) are even higher in energy. There is very little interaction between the 4s and 4p orbitals of iron and the ligand basis orbitals due to the large energy of separation between them. In future figures the 4s orbital will be omitted for simplicity.

Examining Figure 2a in detail, we see the 9a₁ orbital on SQ is stabilized by a bonding interaction with the metal to form the 1e and 1a₁ MOs. That stabilization is quite large due to the good overlap between the 3d and 9a₁ orbitals and their proximity in energy. The 3b₁ orbital on the SQ ligands interacts with the 3d orbitals on the metal to form a bonding and an antibonding combination, the 2e and 3e MOs, respectively, as well as the nonbonding orbital, the a₂ MO. The 3d orbitals on the metal are destabilized by interaction with the σ-bonding SQ orbitals to form a nonbonding metal orbital, the 2a₁ MO. The 7b₂ orbital on SQ and the 3d orbitals interact to form a bonding (not shown) and an antibonding (4e) MO. The highest occupied molecular orbital (HOMO) in Figure 2a is the ligand-delocalized a₂ MO. The HOMO–LUMO separation is not large but is substantially larger than for the analogous chromium complex.[10]

The electronic configuration shown in Figure 2a is for an S = 0 state.

The two lowest energy electronic configurations for an S = 1 state are shown in Figure 2b,c, corresponding to removing

an electron from the 2a₁ and a₂ MOs, respectively, and placing it in the 3e MO. A comparison of Figure 2b with Figure 2a reveals that the 3d orbitals of iron have been substantially stabilized while the SQ orbitals remain essentially unaffected. The stabilization of the 3d orbitals leads to a stabilization of those molecular orbitals in which they participate, namely, the 2e, 3e, 4e, and especially the 2a₁ MOs. In contrast to the situation in Figure 2b, removing an electron from the a₂ MO and placing it into the 3e MO cause a destabilization of the 3d orbitals of iron as may be seen by a comparison of Figure 2c with Figure 2a. This destabilization of the 3d orbitals leads to a destabilization of the 2e, 2a₁, 3e, and 4e MOs and brings about an inversion in the order of the a₂ and 2a₁ MOs, although they are so close energetically they should be considered to be accidentally degenerate.

The results of our calculations on the lowest energy electronic configuration corresponding to an S = 2 state are shown in Figure 2d. An electron has been promoted to the 3e MO from both the 2a₁ and a₂ MOs. The 3d orbitals of iron are stabilized while the ligand basis orbitals remain essentially unchanged, as a comparison of Figure 2d with Figure 2a reveals. The 3d orbitals are not stabilized as much as they are for the $(2a_1)^1(a_2)^2(3e)^1$ configuration, and the accompanying stabilization of the 2e, 2a₁, 3e, and 4e MOs is also smaller than in the $(2a_1)^1(a_2)^2(3e)^1$ case.

The trend in the stability of the 3d orbitals of iron follows the trend in the charge on the iron center. In those configurations where we are taking electron density from the metal-centered 2a₁ MO (i.e., Figure 2b,d) and placing it in the metal–ligand delocalized 3e MO, the positive charge on iron increases and the 3d orbitals are stabilized. The 3d orbitals in the $(2a_1)^1(a_2)^1(3e)^2$ configuration are less stable than in the

Table I. Alternative Configurations

complex	config	S^a	$\tilde{E}_T,^b$ eV
$Fe(SQ)_3^0$	$(2a_1)^2(a_2)^2(3e)^0$	0	-81.30
	$(2a_1)^1(a_2)^2(3e)^1$	1	-81.70
	$(2a_1)^2(a_2)^1(3e)^1$	1	-77.92
	$(2a_1)^1(a_2)^1(3e)^2$	2	-78.89
$Fe(BQ)_3^{3+}$	$(2e)^4(2a_1)^1(a_2)^0(3e)^0$	$^1/_2$	-60.52
	$(2e)^3(2a_1)^1(a_2)^1(3e)^0$	$^3/_2$	-61.93
	$(2e)^2(2a_1)^1(a_2)^1(3e)^1$	$^5/_2$	-60.17
$Fe(CAT)_3^{3-}$	$(2a_1)^2(3e)^3(4e)^0$	$^1/_2$	-71.34
	$(2a_1)^2(3e)^2(4e)^1$	$^3/_2$	-67.85
	$(2a_1)^1(3e)^2(4e)^2$	$^5/_2$	-64.28
$Fe(SQ)_2(CAT)^-$	$(a_2)^2(2a_1)^2(3e)^1$	$^1/_2$	-82.02
	$(a_2)^1(2a_1)^2(3e)^2$	$^3/_2$	-77.26
	$(a_2)^2(2a_1)^1(3e)^2$	$^3/_2$	-83.06
$Fe(SQ)_2(BQ)^+$	$(2a_1)^2(a_2)^1(3e)^0$	$^1/_2$	-74.73
	$(2a_1)^1(a_2)^1(3e)^1$	$^3/_2$	-75.76
$Fe(BQ)_2(SQ)^{2+}$	$(2e)^4(2a_1)^2(a_2)^0(3e)^0$	0	-68.01
	$(2e)^4(2a_1)^1(a_2)^1(3e)^0$	1	-71.61
	$(2e)^3(2a_1)^1(a_2)^1(3e)^1$	2	-70.49

^{a} Total spin for configuration at left. ^{b} Pseudo-total energy defined as an occupation weighted sum of 1-electron eigenvalues for the valence MOs.

$(2a_1)^1(a_2)^2(3e)^1$ configuration because taking an electron from the ligand-delocalized a_2 MO and placing it in the 3e MO, which has significant metal character, partially offset the redistribution of charge from the metal out onto the ligands. This redistribution of charge from the ligands to the metal when an electron is removed from the a_2 MO and placed in the 3e MO is the reason for the destabilization of the 3d orbitals for the $(2a_1)^2(a_2)^1(3e)^1$ configuration.

In order to be able to present a more quantitative measure of the stability of a given configuration, we have defined a "pseudo-total energy", $\tilde{E}_T$, to be an occupation-weighted sum of the 1-electron eigenvalues of the valence MOs.[18] Our approach to the question of what the lowest energy electronic configuration is will be to use the experimental information for the neutral complexes as a guide to interpret the $\tilde{E}_T$'s and use the same interpretation for all other members of the redox series considered here.

The occupation-weighted sums of valence MO eigenvalues for a number of alternative electronic configurations for a representative sampling of the members of the redox series considered here are given in Table I. A given state 1 is lower in energy (and hence more stable) than a state 2 if the magnitude of the $\tilde{E}_T$ for state 1 is larger than that for state 2, i.e., if the value of $\tilde{E}_T$ for state 1 is more negative than the value of $\tilde{E}_T$ for state 2. For the moment we will restrict ourselves to a consideration of the $\tilde{E}_T$'s for the neutral $Fe(SQ)_3$ complex. As might have been expected, the stabilization of the MOs with significant metal character for the $(2a_1)^1(a_2)^2(3e)^1$ configuration as compared to their destabilization for the $(2a_1)^2(a_2)^1(3e)^1$ configuration leads to the $\tilde{E}_T$ value for the former configuration being lower than for the latter. Interestingly, the $\tilde{E}_T$ for the $(2a_1)^1(a_2)^2(3e)^1$ configuration is also lower than than that of the $S = 0$ state. The $\tilde{E}_T$ value for the $S = 2$ state is 2.8 eV higher than the $\tilde{E}_T$ value for the lower energy $S = 1$ state.

The Fenske–Hall method utilizes a spin-restricted formalism so that the increase in exchange energy for an $S = 2$ state over an $S = 1$ state is not taken into account explicitly. The ex-

perimental data provide us with a means of estimating the magnitude of the exchange energy difference. The magnetic susceptibility data summarized earlier suggest the [Fe(3,5-DBSQ)$_3$] complex has an $S = 1$ ground state, while the [Fe(9,10-phenSQ)$_3$] and [Fe(*o*-Cl$_4$SQ)$_3$] complexes have contributions from molecules in higher S states at room temperature.[3] Because the main difference in our calculations on unsubstituted *o*-quinone complexes and 3,5-dialkyl-substituted *o*-quinone complexes is a uniform shift of all MOs to higher energy,[19] which would not affect the difference between the $\tilde{E}_T$'s, our calculations should most closely correspond to the 3,5-DBSQ results. Thus we conclude that a positive energy difference of 2.8 eV in $\tilde{E}_T$ is too large to be overcome in the unsubstituted or 3,5-di-*tert*-butyl-substituted *o*-quinone complexes by the increased exchange energy for an increase in S of 1, but such a difference is not too large to be overcome by the increased exchange energy for the 9,10-phenQ and *o*-Cl$_4$Q ligands.

Applying this interpretation of the $\tilde{E}_T$'s to the rest of Table I, we turn our attention first to [Fe(BQ)$_3$]$^{3+}$. As the table shows, the $S = {}^3/_2$ state is lower in energy than the $S = {}^1/_2$ state and the $S = {}^5/_2$ state is higher in energy than the $S = {}^3/_2$ state by only 1.76 eV. This difference is well below the difference in the neutral case for which the 9,10-phenQ ligands show a population of the higher spin state. Thus, we would be led to predict the $S = {}^5/_2$ state would be the ground state for a 9,10-phenBQ complex, in excellent agreement with the magnetic susceptibility results described earlier. Our experience with the magnitude of exchange energies obtained by simple crystal field theory arguments[10] leads us to favor an $S = {}^5/_2$ ground state for the BQ complex as well, which fits nicely with the high-spin Fe(III) and three-BQ-ligand interpretation of this complex advanced by analogy with the related chromium system.

The last system for which experimental data exist is the [Fe(CAT)$_3$]$^{3-}$ complex. Figure 2 shows the 3e and 4e MOs are well separated. Energetically our calculations give a separation of 4.8 eV between the occupied 3e MO and vacant 4e MO for the $(2a_1)^2(3e)^3(4e)^0$ configuration of the [Fe(CAT)$_3$]$^{3-}$ complex. Table I shows the $S = {}^3/_2$ state to be higher in energy than the $S = {}^1/_2$ state by ~3.5 eV, and the $S = {}^5/_2$ state is even higher in energy, with the $S = {}^1/_2$, $S = {}^5/_2$ difference being ~7.1 eV. This result is understandable from charge considerations. In the neutral and 3+ complexes charge is being taken from metal-centered orbitals and given to primarily ligand-delocalized orbitals, stabilizing all metal levels. For the 3− complex, the electrons are being promoted from metal-centered orbitals to metal-centered orbitals and the stabilization is far less dramatic. For these reasons, we prefer an $S = {}^1/_2$ description for the ground state of the 3− complex. This prediction is at odds with the magnetic susceptibility results mentioned earlier. However, as evidenced by the different values quoted earlier for the [Fe(3,5-DBSQ)$_3$] complex, the value of the magnetic susceptibility of these complexes can be ambiguous, possibly owing to the presence of ferromagnetic iron impurities, which could give larger values for the magnetic susceptibility. We feel the magnetic susceptibility of the 3− complex warrants a reinvestigation in view of the results of our calculations.

For those complexes which are as yet uncharacterized the results in Table I are consistent with an interpretation of this redox series as a high-spin Fe(III) antiferromagnetically coupled to three SQ ligands, with oxidation or reduction of

(18) In so doing, we assume that all other occupied MOs are unchanged by the electron redistributions considered here and hence their eigenvalues remain constant. We believe this approach to be valid because it is the valence orbitals that affect the chemistry of these complexes. Summing a large number of minor changes in the energies of the lower lying molecular orbitals (due to minor variations in the approximate Fock matrix) can tend to obscure the information provided by the orbitals most closely associated with the chemical behavior of these systems, namely, the valence orbitals.

(19) We have performed calculations using the 3,5-dimethyl-1,2-benzoquinone ligand for the iron systems as we did for the chromium system. The results are virtually identical with those for the chromium system. For a discussion of the transferability of the results of our calculations on unsubstituted systems to the larger, substituted, systems see the Appendix in ref 10.

Figure 3. Molecular orbital diagrams for seven-membered redox series of tris(o-quinone)iron complexes. The electronic configuration of the ground state is shown schematically by arrows representing electrons. Arrows with the same direction represent electrons having the same spin. All levels below those containing arrows are completely filled. See test for an explanation of the ligand abbreviations. Where an e label appears without (1) or (2) appended, the MO is doubly degenerate.

the neutral complex leaving the configuration of the metal unchanged and the removed or added electron oxidizing or reducing one of the ligands decoupling it from the metal. Thus, the ground-state configuration for the $[Fe(SQ)_2(CAT)]^-$ complex is predicted to be $(a_2)^2(2a_1)^1(3e)^2$ while that for $[Fe(SQ)_2(BQ)]^+$ complex is predicted to be $(2a_1)^1(a_2)^1(3e)^1$. The difference between the $S = 1$ and $S = 2$ states for the $[Fe(BQ)_2(SQ)]^{2+}$ complex is only 1.1 eV, which leads us to favor the $S = 2$ state as the ground state. Reasoning analogous to that used in the $[Fe(CAT)_3]^{3-}$ case leads one to conclude the $(2a_1)^1(3e)^2(4e)^1$ configuration is much higher in energy than the $(2a_1)^2(3e)^2(4e)^0$ configuration because the electron is promoted from a metal-centered to a metal-centered MO, and we favor the $S = 1$ state as the ground state for this complex.

$Fe(Q)_3{}^n$ ($n = 3+, ..., 3-$) ($Q = o$-Quinone). Figure 3 presents the results of our calculations on the seven-membered redox series of tris(o-quinone)iron complexes with overall charges ranging from 3+ to 3−. The symmetry labels for the ligand basis orbitals are as in Figure 2 with the ligand type appearing below. Thus, where a BQ is added, this means that the orbital comes from a quinone ligand whose iron–oxygen, oxygen–carbon, and carbon–carbon bond distances and angles correspond to an o-benzoquinone type ligand while SQ significes the orbital is from a semiquinone ligand and CAT means that the basis orbital is obtained from a catecholate

ligand. The symmetry labels for the MOs are taken from the D_3 point group as earlier and are analogous to those in Figure 2 except the "2" has been dropped from $2a_1$ for compactness. The MO labels have been assigned in those complexes with symmetry lower than D_3 by analogy for ease of comparison. Where the degenerate e levels are split due to the lower symmetry, a (1) or (2) is attached to the label to identify the components. MOs corresponding to the 1e, $1a_1$, and 4e MOs in Figure 2 have been omitted for the sake of simplicity because their energies relative to the ligand (1e, $1a_1$) or metal (4e) levels remain essentially unchanged and their inclusion adds nothing to the present discussion. The electronic configurations used are as discussed above and are represented schematically as in Figure 2.

An examination of Figure 3 reveals that, as we start on the left side of the figure with the 3+ complex and proceed to the right, the 3d orbitals are destabilized relative to the ligand orbitals. In Figure 3a the 2e MO is mainly metal in character while the 3e MO is mainly ligand in character, giving an ionic description of the bonding between metal and ligands. As we reduce the 3+ complex and the 3d orbitals are destabilized relative to the ligand orbitals, the bonding becomes more covalent, with roughly equal ligand and metal character in the 2e and 3e MOs in Figure 3e,f. Further reduction leads once again to a more ionic bonding picture with the 2e MO now being mainly ligand in character and the 3e MO mainly metal

Table II. Charges on the Complex Fragments

	Mulliken charges[a]			
complex	Fe	BQ	SQ	CAT
Fe(BQ)$_3$$^{3+}$	1.59+	0.47+		
Fe(BQ)$_2$(SQ)$^{2+}$	1.60+	0.16+	0.07+	
Fe(SQ)$_2$(BQ)$^+$	1.60+	0.13–	0.24–	
Fe(SQ)$_3$	1.66+		0.55–	
Fe(SQ)$_2$(CAT)$^-$	1.64+		0.83–	0.98–
Fe(CAT)$_2$(SQ)$^{2-}$	1.55+		1.10–	1.23–
Fe(CAT)$_3$$^{3-}$	1.44+			1.47–

[a] Based upon a Mulliken population analysis. Charges for the ligands are relative to a neutral $O_2C_6H_4$ molecular fragment.

in character in Figure 3g. The a_1 MO follows the trend of the destabilization in the 3d orbitals of iron while the nonbonding ligand-delocalized a_2 MO remains relatively unchanged; this brings about an inversion of their ordering upon going from the 1– to the 2– complexes.

As in the chromium series, because the o-quinone ligands themselves exhibit a variety of oxidation states, the question of what are the preferred descriptions of the metal and ligand oxidation states naturally arises. To address the problem of the metal and ligand oxidation states, we present the results of a Mulliken population analysis[20] on our molecular orbitals for the seven-membered redox series of iron complexes in Table II. The charges given in the table are relative to the neutral atom or ligand. Thus, the charge on uncomplexed BQ would be 0+, while the charge on free SQ would be 1– and uncomplexed CAT would carry a 2– charge. The most striking feature about Table II is the trend in the charge on iron over the seven-membered redox series. As in the analogous chromium series, over the span of a 6-unit change in the overall charge on the complex regardless of whether the added electron occupies a metal-centered, ligand-delocalized, or metal–ligand-delocalized MO, the charge on iron changes only slightly, i.e., by only 0.22 of an electron. Initially, although the overall charge on the complex decreases as we go down the table, the charge on iron remains nearly constant or increases slightly, reaching a maximum at the neutral species. Thereafter, the charge on iron decreases, but by much less than the unit of charge that is added. As was the case for the related chromium series, the explanation for the small changes in the iron charge lies in an examination of the changes in the metal–ligand bonding that occur as the complexes undergo reduction. There is a substantial change in the percent character of the metal and ligand basis orbitals in the MOs due to changes in the relative energies of the metal and ligand basis orbitals as a given member of the series is reduced. Because of the changing character of the MOs, regardless of whether the electron is added to a ligand- or metal-centered orbital, the charge is mostly redistributed out onto the ligands.

There are two points worth noting about the charges on the ligands in Table II. First, it can be seen that the charges on the ligands usually deviate substantially from what we might expect on the basis of the uncomplexed ligand. Second, in those cases where two different types of quinone ligand are present in the same complex (e.g., [Fe(SQ)$_2$(BQ)]$^+$), a comparison reveals that the charge on the BQ is always more positive than the charge on SQ and the charge on SQ is always more positive than that on CAT. Thus, even though the ligand charges differ substantially from those of the free ligands, their relative magnitudes are what we would expect, just as in the chromium system.

On the basis of the spectral and structural information reviewed earlier the 3+, neutral, and 3– iron tris(o-quinone) complexes have been formulated as an Fe^{3+} bonded to three

Table III. Comparison of UV–Visible Spectral Transition Energies[a]

| calcd			obsd			
complex	transition	ΔE, eV	complex	λ_{max}, nm	ΔE, eV	ref
Fe(CAT)$_3$$^{3-}$	$a_2 \rightarrow 3e$	2.9	Fe(CAT)$_3$$^{3-}$	560	2.2	2
	$2e \rightarrow 3e$	3.3		~495	2.5	9, 17, 21
	$1a_1 \rightarrow 3e$	4.3		330	3.8	21
				290	4.3	21
			Fe(o-Cl$_4$CAT)$_3$$^{3-}$	620	2.0	22
				540	2.3	22
Fe(SQ)$_3$	$2a_1 \rightarrow 3e$	1.7	Fe(3,5-DBSQ)$_3$	650	1.9	2
	$2e \rightarrow 3e$	2.7		430	2.9	2
	$1a_1 \rightarrow 2a_1$	2.9		375	3.3	2
	$1e \rightarrow 2a_1$	3.0		300	4.1	2
	$1a_1 \rightarrow 3e$	4.6				
Fe(BQ)$_3$$^{3+}$	$1e \rightarrow 2e$	1.6	b			
	$1a_1 \rightarrow 2e$	1.8				
	$2a_1 \rightarrow 3e$	3.9				
	$2e \rightarrow 3e$	4.0				

[a] Calculated transition energies in the UV–visible range for the 3+, neutral, and 3– iron complexes in eV are compared with literature values for known complexes. [b] No UV–visible data are available on a 3+ iron complex.

o-benzoquinone, o-semiquinone, and catecholate ligands, respectively. While our charge for iron differs substantially from 3+, we are in basic agreement with the supposition that the charge on the iron remains essentially constant over the entire seven-membered series while the charge is added to or subtracted from the ligands; this result is entirely analogous to that obtained from our calculations on the related chromium system.

The UV–visible spectra for several iron complexes of the type discussed here have been previously reported.[2,9,17,21,22] Transition energies in electronvolts for the low-energy electronic transitions obtained from our calculations on the [Fe-(CAT)$_3$]$^{3-}$, [Fe(SQ)$_3$], and [Fe(BQ)$_3$]$^{3+}$ complexes along with the assignments of these transitions are summarized in Table III and are compared to literature values for known complexes. The calculated values were obtained by taking the difference in the 1-electron eigenvalues of the levels involved from the ground-state calculation; this does not take into account changes that occur in the Coulomb and exchange integrals in the excited configuration.[23] Despite the simplicity of the model and the approximate nature of the calculations, the correlation between the calculated and observed values is surprisingly good. All experimental values reported have extinction coefficients of at least 4000 M^{-1} cm^{-1} and have been assigned as either metal to ligand or ligand to metal charge-transfer bands. The transitions in the calculated energies are all one of these types and are spin allowed and hence would be expected to show large extinction coefficients. No visible spectra on a compound of tris(benzoquinone) type have been reported although [Fe(9,10-phenBQ)$_3$]Br$_3$ is reported to be a brown, crystalline solid.[7]

Comparison of Fe and Cr. In order to compare our results on the iron and chromium systems, we present a representative

(20) Mulliken, R. S. *J. Chem. Phys.* **1955**, *23*, 1841–1846.

(21) Salama, S.; Stong, J. D.; Neilands, J. B.; Spiro, T. G. *Biochemistry* **1978**, *17*, 3781–3785.

(22) Abakumova, L. G.; Domrachev, G. A.; Abakumov, G. A. *J. Gen. Chem. USSR (Engl. Transl.)* **1974**, *44*, 793–796; *Zh. Obshch. Khim.* **1974**, *44*, 823–826.

(23) Transition energies calculated in this manner between occupied and virtual MOs obtained from Fenske–Hall calculations generally give extremely poor quantitative agreement with experiment. This is because the virtual orbitals obtained from Fenske–Hall calculations are usually too high in energy. All transitions considered in the present case are from partially or fully occupied MOs to partially occupied MOs, and this might explain the surprisingly good quantitative agreement in this instance.
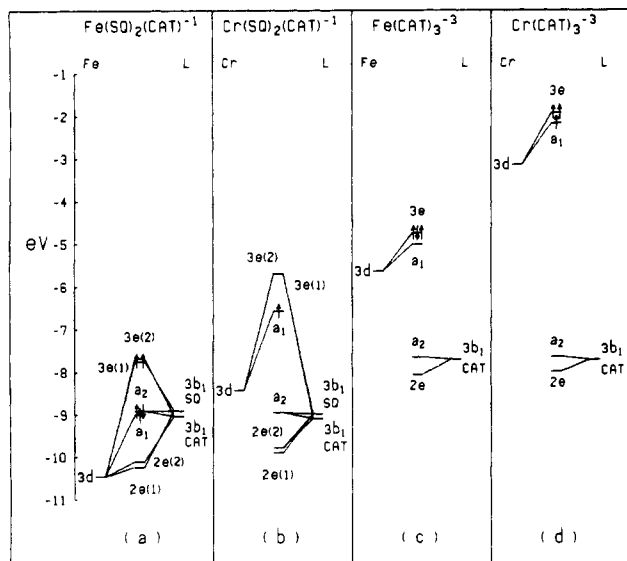
Figure 4. Molecular orbital diagrams comparing iron and chromium complexes. The electronic configuration is shown schematically by arrows representing electrons. Arrows having the same direction represent electrons with the same spin. All levels below those containing arrows are completely filled. Where an e label appears without (1) or (2) appended, the MO is doubly degenerate.

sample of MO diagrams for the iron and chromium complexes with overall charges of 1– and 3– in Figures 4. The symmetry labels for the iron complexes are as in Figure 3, and the electronic configuration is presented schematically as previously described. The 2e and 3e MOs for the chromium complexes are the same as the 1e and 2e MOs, respectively, in ref 10 and have been relabeled so as to correspond with the iron labels in Figure 3.

If we compare the complexes with like overall charges, consideration of Figure 4a,b reveals that the 3d orbitals of Fe are more stable relative to the ligand levels than are the 3d orbitals of Cr. The iron complex contains 2 extra electrons, which populate the 3e level. The a_2 MO is at virtually the same energy for either complex but due to the stability of the iron 3d orbitals the a_1 and 3e MOs bracket the a_2 MO for the $[Fe(SQ)_2(CAT)]^-$ complex while the a_1 and 3e MOs lie well above the a_2 MO for the $[Cr(SQ)_2(CAT)]^-$ complex. The a_1 and 3e MOs are not so strongly destabilized in the iron 1– complex as they are in the chromium 1– complex, which probably reflects a slightly weaker metal–ligand interaction due to the longer metal–oxygen bond length in the iron system. A comparison of Figure 4c with Figure 4d reveals that the 3– complexes have the same basic features. Because the 3d orbitals of iron are more stable than the 3d orbitals of chromium and the $3b_1$ orbital on the CAT ligand is at roughly the same energy for both complexes, the energy difference between the ligand-delocalized 2e and a_2 MOs and the metal-localized a_1 and 3e MOs is smaller for the $[Fe(CAT)_3]^{3-}$ complex than it is for the $[Cr(CAT)_3]^{3-}$ complex. This difference in the energy gap between the ligand- and metal-centered MOs for the iron and chromium complexes is reflected in differences in their electronic spectra. Recall from Table III that the iron 3– complex exhibits an intense absorption in the visible region of the spectrum assignable to a ligand to metal charge-transfer transition. The visible spectrum of the chromium 3– complex[13] contains no intense bands assignable to charge-transfer transitions and is characteristic of a spectrum containing d → d transitions only. That the iron 3– complex should and the chromium 3– complex should not have low-energy charge-transfer type transitions in the visible region of the spectrum is brought out nicely by a comparison of Figure 4c with Figure 4d.

In a comparison of complexes that are isoelectronic, a consideration of Figure 4a with Figure 4d brings out more dramatically the greater stability of the 3d orbitals of iron as compared to the 3d orbitals of chromium. In $[Cr(CAT)_3]^{3-}$ the bonding is essentially ionic with the 2e MO being almost entirely ligand in character and the 3e MO being almost exclusively metal in character. In contrast to this, the bonding in $[Fe(SQ)_2(CAT)]^-$ is largely covalent with the 2e and 3e MOs containing substantial contributions from both ligand and metal orbitals. To address the problem of the relative stabilities of the iron and chromium complexes, a comparison of Figure 4a with Figure 4d provides no evidence for the iron complex being less stable than the chromium complex for these isoelectronic species. On the contrary, the occupied MOs are considerably lower in energy for the iron complex than they are for the chromium complex. One may reasonably conclude from the diagram that, if the chromium 3– complex were to exist, thermodynamically there is no reason that an iron 1– complex should not exist.

Finally, consider a comparison of Figure 4b with Figure 4c. Note how the separation between the 2e and a_2 MOs and the a_1 and 3e MOs is similar for the chromium 1– and iron 3– complexes, despite the fact that the iron complex contains 4 more electrons than the chromium complex. The visible spectrum of the $[Cr(3,5\text{-}DBQ)_3]^-$ complex exhibits a broad, complicated band between 550 and 650 nm,[13] which compares favorably with the visible absorption bands for iron 3– complexes given in Table III. Thus, from an electronic spectral point of view, the iron complexes behave like the chromium complexes having 4 less electrons.

Summary

We have presented the results of Fenske–Hall calculations on a seven-membered redox series of tris(*o*-quinone)iron complexes and have compared them to the related chromium series. Using a "pseudo-total energy" defined as an occupation-weighted sum of the 1-electron eigenvalues of the valence MOs and magnetic susceptibility results, we have made predictions of the electronic configuration of the ground state for each member of the series. We postulate there should be 5, 4, 3, 2, and 3 unpaired electrons for the ground state of the 3+, 2+, 1+, neutral, and 1– iron complexes, respectively, due to a stabilization of all MOs involving metal 3d orbitals when the electrons are unpaired. For the 2– and 3– iron complexes we conclude there should only be 2 and 1 unpaired electrons, respectively, due to the large 3e–4e energy separation and the lack of stabilization of the MOs by such metal-localized orbital to metal-localized orbital electron promotions. Our result for the 3– iron complex is at odds with the magnetic data that have been reported for this complex, but we believe our results warrant a further investigation of the magnetic susceptibility of this species.

For the entire seven-membered redox series, the destabilization in the 3d orbitals of iron relative to the ligand orbitals is quite dramatic and is analogous to the chromium series. Beginning with the 3+ iron complex, we find the 2e MO is primarily metal in character, the 3e MO is primarily ligand in character, and the bonding description is essentially ionic. As the complexes are reduced, a smooth transition to a more covalent type of bonding occurs with the 2e and 3e MOs having large metal and ligand contributions for the 1– and 2– complexes. As these complexes are further reduced, the bonding once again becomes ionic with the 2e MO now mainly ligand in character and the 3e MO now mainly metal in character. The charge on iron changes very little over the entire seven-membered series and is entirely analogous to the trend in charges for the related chromium system. Our calculations are consistent with a model for these complexes in which the charge on iron remains essentially constant over the

entire series and electrons are added to or taken from the ligands. The results of our calculations are in good agreement with the qualitative and quantitative aspects of the UV–visible spectra of tris(*o*-quinone)iron complexes considering the approximate nature of the Fenske–Hall method.

In a comparison of the iron series to the related chromium series, we have found that in complexes with the same overall charge but different metals the 3d orbitals of iron are more stable than the 3d orbitals or chromium. The iron-ligand interactions appear to be slightly weaker than the chromium–ligand interactions, which is probably due to the longer Fe–O bond lengths. When isoelectronic complexes of iron and chromium are compared, the greater stability of the 3d orbitals of iron is even more pronounced. The MOs for the isoelectronic iron 1– and chromium 3– complexes are much lower in energy for the iron complex than for the chromium complex and such a comparison provides no support for any supposed lesser stability of the iron 1– compound as compared to the chromium 1– compound. The inability to obtain evidence for the existence of an iron 1– complex may very well be related to a kinetic as opposed to a thermodynamic instability, as has been previously suggested.[3] Comparison of our calculations on the 3– complexes of iron and chromium provides convincing

evidence for the presence and lack of an intense transition in the visible region of the spectrum assignable to a ligand to metal charge-transfer transition for the iron and chromium complexes, respectively. The iron system is analogous in many ways to the chromium system presented earlier. However, it has been pointed out that from a bonding and energetic point of view a given iron complex most closely resembles a chromium complex containing 4 fewer electrons rather than the isoelectronic chromium complex. As in the chromium series, the dramatic changes in the bonding over the entire seven-membered redox series are directly attributable to the dramatic destabilization of the 3d orbitals of iron as the complexes are reduced.

Registry No. Fe(BQ)$_3^{3+}$, 81875-94-7; Fe(BQ)$_2$(SQ)$^{2+}$, 81875-95-8; Fe(SQ)$_2$(BQ)$^+$, 81875-96-9; Fe(SQ)$_3$, 81857-50-3; Fe(SQ)$_2$(CAT)$^-$, 81875-92-5; Fe(CAT)$_2$(SQ)$^{2-}$, 81875-93-6; Fe(CAT)$_3^{3-}$, 67966-15-8.

Contribution from the Commissariat à l'Energie Atomique, Centre d'Etudes Nucléaires, Section des Transuraniens, 92260 Fontenay-aux-roses, France, and Laboratoire de Chimie des Métaux de Transition, Université Pierre et Marie Curie, 75230 Paris Cedex 05, France

Spectrophotometric Identification of a Mixed-Valence Cation–Cation Complex between Aquadioxovanadium(V) and Aquaoxovanadium(IV) Ions in Perchloric, Sulfuric, and Hydrochloric Acid Media

P. BLANC,[1a] C. MADIC,*[1a] and J. P. LAUNAY[1b]

The mixture of aquadioxovanadium(V) and aquaoxovanadium(IV) ions in perchloric, sulfuric, and hydrochloric acid media gives a mixed-valence cation–cation 1/1 complex, V$_2$O$_3^{3+}$(aq), which was studied by absorption spectrophotometry. The order of stability of V$_2$O$_3^{3+}$(aq) vs. the nature of the medium is H$_2$SO$_4$ > HClO$_4$ > HCl for acid concentrations lower than 8 M. In perchloric acid (8.7 M) the formation constant is found, K = 8.1 M^{-1} (σ_K = 1.3%), whereas in 5 N HClO$_4$, K is lower and estimated to be about 0.8 M^{-1}; for this medium the thermodynamic parameters ΔH = −10.0 ± 0.8 kJ mol^{-1} and ΔS = −35.5 ± 4.2 J mol^{-1} K^{-1}. These characteristics are very close to those of cation–cation complexes involving actinide(V) ions (MO$_2^+$). The electronic spectrum of V$_2$O$_3^{3+}$(aq) presents an intense absorption for the whole visible range characterized by four transitions (17 500, 15 150, 12 300, and 10 100 cm^{-1}). The transition located at ν = 10 100 cm^{-1} can be attributed to intervalence band transition.

Introduction

A special feature of the chemistry of pentavalent actinides is the property of MO$_2^+$ ions (where M = actinide) to form "cation–cation" complexes with certain cations in acidic noncomplexing (ClO$_4^-$) or slightly complexing (Cl$^-$, NO$_3^-$) aqueous solutions. The first term of the series, Np(V)–U(VI), was identified by Sullivan[2] by means of spectrophotometric and potentiometric measurements, and since then, it has been shown that U(V), Pu(V), and Am(V) possessed the same property.[3] The nature of these "cation–cation" complexes is a subject of controversy. Sullivan and most workers consider

them as true complexes, while Rykov and others feel that these species correspond rather to "long-range" interactions of the "aborted" redox reaction type, involving solvent molecules.[3a] However additional proofs of the existence of these complexes were provided recently: (1) It was confirmed by absorption spectrophotometry that the formation of the complexes Np-(V)–U(VI), Np(V)–Np(VI), and Am(V)–U(VI) obeys the law of mass action.[3b,4] (2) Raman spectrometry has revealed a modification in the M–O bond (of the MO$_2^+$ ion) during complexation of NpO$_2^+$ by U(VI) and Np(V) and that of AmO$_2^+$ by U(VI).[5] (3) X-ray diffraction was used to measure the distance between metallic nuclei in solutions containing the complexes Np(V)–U(VI) and Np(V)–Np(V).[6]

(1) (a) Centre d'Etudes Nucléaires. (b) Université Pierre et Marie Curie.
(2) Sullivan, J. C.; Hindman, J. C.; Zielen, A. J. *J. Am. Chem. Soc.* **1961**, *83*, 3373.
(3) For further information, see: (a) Frolov, A. A.; Rykov, A. G. *Radiokhimiya* **1979**, *3*, 329. (b) Madic, C.; Guillaume, B.; Morisseau, J.-C.; Moulin, J.-P. *J. Inorg. Nucl. Chem.* **1979**, *41*, 1027.

(4) Guillaume, B.; Hobart, D.; Hahn, R. L.; Bourges, J. *J. Inorg. Nucl. Chem.*, in press.
(5) Guillaume, B.; Begun, G. M.; Hahn, R. L.; Narten, A. H. "11 èmes Journées des Actinides"; Jesolo Lido: Venice, Italy, 1981.